

2

Population Codes

3

4 *Alexandre Pouget and Peter E. Latham*

5 Introduction

6 Many sensory and motor variables in the brain are encoded by
7 coarse codes, i.e., by the activity of large populations of neurons
8 with broad tuning curves. For example, the direction of visual
9 motion is believed to be encoded in the medial temporal (MT) visual
10 area by a population of cells with bell-shaped tuning to direction,
11 as illustrated in Figure 1A. Other examples of variables encoded
12 by populations include the orientation of a line, the contrast in a
13 visual scene, the frequency of a tone, and the direction of intended
14 movement in motor cortex. These encodings extend to two
15 dimensions—a single set of neurons might contain information
16 about both orientation and contrast—or more.

17 Population codes are computationally appealing for at least two
18 reasons. First, the overlap among the tuning curves allows precise
19 encoding of values that fall between the peaks of two adjacent
20 tuning curves (Figure 1A). Second, bell-shaped tuning curves provide
21 basis functions that can be combined to approximate a wide
22 variety of nonlinear mappings. This means that many cortical
23 functions, such as sensorimotor transformations, can be easily modeled
24 with population codes (see Pouget, Zemel, and Dayan, 2000, for a
25 review).

26 In this article we focus on decoding, or reading out, population
27 codes. Decoding is the simplest form of computation that one can
28 perform over a population code, and as such, it is an essential step
29 toward understanding more sophisticated computations. It is also
30 important for accurately identifying which variables are encoded
31 in a particular brain area and how they are encoded.

32 A key element of population codes—and the main reason why
33 decoding them is difficult—is that neuronal responses are noisy,
34 meaning that the same stimulus can produce different responses.
35 Consider, for instance, a population of neurons coding for a one-
36 dimensional parameter: the direction, θ , of a moving object. An
37 object moving in a particular direction produces a *noisy* hill of
38 activity across this neuronal population (Figure 1C). On the basis
39 of this noisy activity, one can try to come up with a good guess,
40 or estimate, $\hat{\theta}$, of the direction of motion, θ . In the second and third
41 sections of this article we review the various estimators that have
42 been proposed, and in the fourth section we consider their neuronal
43 implementations.

44 Additional sources of uncertainty, beside neuronal noise, can
45 come from the variable itself. For example, there is intrinsically
46 more variability in one's estimate of, say, motion on a dark night
47 than motion in broad daylight. In cases such as this, it is not un-
48 reasonable to assume that population activity codes for more than
49 just a single value, and in the extreme case the population activity
50 could code for a whole *probability distribution*. The goal of de-
51 coding is then to recover an estimate of this probability distribution.
52 We consider an example of this later in the article.

53 Models of Neuronal Noise and Tuning Curves

54 To read a population code, it is essential to have a good under-
55 standing of the relation between the patterns of activity and the
56 encoded variables. One common assumption, particularly in sensory
57 and motor cortex, is that patterns of activity encode a single
58 value per variable at any given time. This is a reasonable assump-
59 tion in many situations (although there are exceptions, as discussed
60 later). For example, an object can move in only one direction at a
61 time, so the neurons encoding its direction of motion have only
62 one value to encode.

63 Under the assumption of a single value, neuronal responses are
64 generally characterized by tuning curves, noted $f_i(\theta)$, which specify
65 the mean activity of cell i as a function of the encoded variable.
66 These tuning curves are typically bell-shaped, and are often taken

67 to be Gaussian for nonperiodic variables and circular normal for
68 periodic ones.

69 Simply measuring the mean activity, however, is not sufficient
70 for performing estimation. A neuron may fire at a rate of 20 spikes/
71 s on one trial but only 15 spikes/s on the next, even though the
72 same stimulus was presented both times. This trial-to-trial vari-
73 ability is captured by the noise distribution, $P(a_i = a|\theta)$, where a_i
74 is the activity of cell i . The noise distribution is often assumed to
75 be Gaussian, either with fixed variance or with a variance propor-
76 tional to the mean (the latter being more consistent with experi-
77 mental data), and independent. Such a distribution has the form

$$78 \quad P(a_i = a|\theta) = \frac{1}{\sqrt{2\pi\sigma_i^2}} \exp\left(-\frac{(a - f_i(\theta))^2}{2\sigma_i^2}\right) \quad (1)$$

79 where σ_i^2 is either fixed or equal to the mean, $f_i(\theta)$. Another popular
80 choice, especially useful if one is counting spikes, is the Poisson
81 distribution:

$$82 \quad P(a_i = k|\theta) = \frac{f_i(\theta)^k e^{-f_i(\theta)}}{k!} \quad (2)$$

83
84
85 Figure 1C shows a typical pattern of activity with Gaussian noise
86 and σ_i^2 fixed.

87 Estimating a Single Value

88 We now consider various approaches to reading out a population
89 code under the assumptions that (1) a single value is encoded at
90 any given time, and (2) the only source of uncertainty is the neu-
91 ronal noise. Most of these methods, known as estimators, seek to
92 recover an estimate, $\hat{\theta}$, of the encoded variable. We first discuss
93 how one assesses the quality of an estimator in general; we then
94 provide descriptions of common estimators used for decoding
95 population activity.

96 Fisher Information

97 An estimate, $\hat{\theta}$, is obtained by computing a function of the observed
98 activity \mathbf{A} , where $\mathbf{A} = (a_1, a_2, \dots)$. Because of neuronal noise, \mathbf{A}
99 is a random variable and thus so is $\hat{\theta}$. This means that $\hat{\theta}$ will vary
100 from trial to trial even for identical presentation angles. The best
101 estimators are ones that are unbiased and efficient. An unbiased
102 estimator is right on average: the conditional mean, $E[\hat{\theta}|\theta]$, is equal
103 to the encoded direction, θ , where E denotes an average over trials.
104 An efficient estimator, on the other hand, is consistent from trial
105 to trial: the conditional variance, $E[(\hat{\theta} - \theta)^2|\theta]$, is minimal.

106 In general, the quality of an estimator depends on a compromise
107 between the bias and the conditional variance. In this chapter, how-
108 ever, we consider unbiased estimators only, for which the condi-
109 tional variance is the important measure because it fully determines
110 how well one can discriminate small changes in the encoded vari-
111 able based on observation of the neuronal activity. There exists a
112 theoretical lower bound on the conditional variance, which is
113 known as the Cramér-Rao bound. For an unbiased estimator, this
114 bound is equal to the inverse of the Fisher information (Paradiso,
115 1988; Seung and Sompolinsky, 1993) which leads to the inequality

$$116 \quad E[(\hat{\theta} - \theta)^2] \geq \frac{1}{I_{\text{Fisher}}}$$

117 where

$$118 \quad I_{\text{Fisher}} \equiv E\left[-\frac{\partial^2}{\partial\theta^2} \log P(\mathbf{A}|\theta)\right]$$

119
120
121 An efficient estimator is one whose conditional variance is equal
122 to the Cramér-Rao bound, $1/I_{\text{Fisher}}$. When $P(\mathbf{A}|\theta)$ is known, it is
123 often straightforward to compute I_{Fisher} . For example, for the Gaus-
124 sian distribution given in Equation 1,

$$125 \quad I_{\text{Fisher}} = \sum_{i=1}^N \frac{f_i'(\theta)^2}{\sigma_i^2}$$

126 and for the Poisson distribution given in Equation 2,

$$127 \quad I_{\text{Fisher}} = \sum_{i=1}^N f_i'(\theta)^2$$

$$I_{\text{Fisher}} = \sum_{i=1} \frac{1}{f_i(\theta)}$$

130 (Seung and Sompolinsky, 1993).

131 In both of these expressions, the neurons that contribute most
132 strongly to the Fisher information are those with a large slope (large
133 $f_i'(\theta)$). Therefore, the most active neurons are not the most infor-
134 mative ones. In fact, they are the *least* informative: the most active
135 neurons correspond to the top of the tuning curve, where the slope
136 is zero, so these neurons make no contribution to Fisher
137 information.

138 *Voting Methods*

139 Several estimators rely on the idea of interpreting the activity of a
140 cell, normalized or not, as a vote for the preferred direction of the
141 cell. For instance, the optimal linear estimator is given by

$$142 \hat{\theta}_{\text{OLE}} = \sum_{i=0}^N \theta_i a_i$$

144 where θ_i is the preferred direction of cell i , that is, the peak of the
145 function $f_i(\theta)$. A variation on this theme is the center of mass es-
146 timator, defined as

$$147 \hat{\theta}_{\text{COM}} = \frac{\sum_{i=1}^N \theta_i (a_i - \gamma)}{\sum_{i=1}^N (a_i - \gamma)}$$

149 where γ is the spontaneous activity of the cells.

150 A third variation is known as a population vector estimator (Fig-
151 ure 2A). This has been extensively used for estimating periodic
152 variables, such as direction, from real data (Georgopoulos et al.,
153 1982). It is equivalent to fitting a cosine function through the pat-
154 tern of activity and using the phase of the cosine as the estimate of
155 direction:

$$156 \hat{\theta}_{\text{COMP}} = \text{phase}(z)$$

158 where

$$159 z = \sum_{j=1}^N a_j e^{i\theta_j}$$

161 The first two methods work best for nonperiodic variables; the
162 third one can only be used when the variables are periodic. All
163 three estimators are subject to biases, although careful tuning of
164 the parameters can often correct for them. More important, all three
165 methods are almost always suboptimal (the variance of the esti-
166 mator exceeds the Cramér-Rao bound). The exceptions occur for a
167 very specific set of tuning curves and noise distributions (Salinas
168 and Abbott, 1994): the center of mass is optimal only with Gaussian
169 tuning curves and Poisson noise, and the population vector is op-
170 timal only for cosine tuning curves and Gaussian noise of fixed
171 variance.

172 *Maximum Likelihood*

173 A better choice than the voting methods, at least from the point of
174 view of statistical efficiency, is the maximum likelihood (ML)
175 estimator,

$$176 \hat{\theta}_{\text{ML}} = \arg \max_{\theta} P(\mathbf{A}|\theta)$$

178 When there are a large number of neurons, this estimator is un-
179 biased and its variance is equal to the Cramér-Rao bound for a
180 wide variety of tuning curve profiles and noise distribution (Para-
181 diso, 1988; Seung and Sompolinsky, 1993). The term maximum
182 likelihood comes from the fact that $\hat{\theta}_{\text{ML}}$ is obtained by choosing
183 the value of θ that maximizes the conditional probability of the
184 activity, $P(\mathbf{A}|\theta)$, also known as the likelihood of θ .

185 Finding the ML estimate reduces to template matching (Para-
186 diso, 1988), i.e., finding the noise-free hill that is closest to the
187 activity, as illustrated in Figure 2B. If the noise is independent and
188 Gaussian, then “closest” is with respect to the Euclidean norm, $\sum_i (a_i$

189 $- f_i(\theta)^2$. For other distributions the norm is more complicated.
 190 Template matching involves a nonlinear regression, which is typi-
 191 cally performed by moving the position of the hill until the dis-
 192 tance from the data is minimized, as shown in Figure 2B. The
 193 position of the peak of the final hill corresponds to the ML estimate.

194 The main difference between the population vector and the ML
 195 estimator is the shape of the template being matched to the data.
 196 Whereas the population vector matches a cosine, the ML estimator
 197 uses a template that is directly derived from the tuning curves of
 198 the neurons that generated the activity (Figures 2A and 2B). (When
 199 all neurons have identical tuning curves, as for our examples, the
 200 template has the same profile as the tuning curves.) It is because
 201 the ML estimator uses the correct template that its variance reaches
 202 the Cramér-Rao bound. There is, however, a cost: one needs to
 203 know the profile of all tuning curves to use ML estimation, whereas
 204 only the preferred directions, θ_i , are needed for the population vec-
 205 tor estimator.

206 *Bayesian Approach*

207 An alternative to ML estimation is to use the full posterior distri-
 208 bution of the encoded variable, $P(\theta|\mathbf{A})$. This is related to the dis-
 209 tribution of the noise, $P(\mathbf{A}|\theta)$, through Bayes's theorem:

$$210 \quad P(\theta|\mathbf{A}) = \frac{P(\mathbf{A}|\theta)P(\theta)}{P(\mathbf{A})}$$

212 where $P(\mathbf{A})$ and $P(\theta)$ are the prior distributions over \mathbf{A} and θ . The
 213 value that maximizes $P(\theta|\mathbf{A})$ can then be used as an estimate of θ .
 214 This is known as a maximum a posteriori estimate, or MAP esti-
 215 mate. The main advantage of the MAP estimate over the ML esti-
 216 mate is that prior knowledge about the encoded variable can be
 217 taken into account. This is particularly important when the condi-
 218 tional distribution, $P(\mathbf{A}|\theta)$, is not sharply peaked compared to the
 219 prior, $P(\theta)$. This happens, for example, when only a small number
 220 of neurons are available, or when one observes only a few spikes
 221 per neuron. The MAP estimate is close to the ML estimate if the
 222 prior distribution varies slowly compared to the conditional, and
 223 the two are exactly equal when the prior is flat. Several authors
 224 have explored and/or applied applied this approach to real data
 225 (Foldiak, 1993; Sanger, 1996; Zhang et al., 1998).

226 **Neuronal Implementations**

227 Methods such as the voting schemes or ML estimator are biolog-
 228 ically implausible, for one simple reason: they extract a single
 229 value, the estimate of the encoded variable. Such explicit decoding
 230 is very rare in the brain. Instead, most cortical areas and subcortical
 231 structures use population codes to encode variables. This means
 232 that, throughout the brain, population codes are mapped into popu-
 233 lation codes. Hence, V1 neurons, which are broadly tuned to the
 234 direction of motion, project to MT neurons, which are also broadly
 235 tuned, but in neither area is the direction of motion read out as a
 236 single number. The neurons in MT are nevertheless confronted with
 237 an estimation problem: they must choose their activity levels on
 238 the basis of the noisy activity of V1 neurons.

239 What is the optimal strategy for mapping one population code
 240 into another? We cannot answer this question in general, but we
 241 can address it for the broad class of networks depicted in Figure 3.
 242 In these networks, the input layer is a set of neurons with wide
 243 tuning curves, generating noisy patterns of activity like the one
 244 shown in Figure 1C. This activity, which acts transiently, is relayed
 245 to an output layer through feedforward connections. In the output
 246 layer the neurons are connected through lateral connections.

247 An update rule (discussed later) causes the activity in the output
 248 layer to evolve in time. In the next section we consider networks
 249 in which the update rule leads to a smooth hill. The peak of that
 250 hill can be interpreted as an estimate of the variable being encoded.
 251 As previously, we can assess how well the network did by looking
 252 at the mean and variance of this estimate.

253 We will consider two kinds of networks: those with a linear
 254 activation function and those with a nonlinear one.

255 *Linear Networks*

256 We first consider a network with linear activation functions in the
257 output layer, so that the dynamics is governed by the difference
258 equation

$$259 \quad \mathbf{O}_t = ((1 - \lambda)I + \lambda W)\mathbf{O}_{t-1}, \quad (3)$$

261 where λ is a number between 0 and 1, I is the identity matrix, and
262 W is the matrix for the lateral connections. The activity at time 0,
263 \mathbf{O}_0 , is initialized to $W\mathbf{A}$, where \mathbf{A} is an input pattern (like the one
264 shown in Figure 1C) and W is the feedforward weight matrix (for
265 simplicity, the feedforward and lateral weights are the same, al-
266 though this is not necessary).

267 The dynamics of such a network is well understood: each eigen-
268 vector of the matrix $(1 - \lambda)I + \lambda W$ evolves independently, with
269 exponential amplification for eigenvalues greater than 1 and ex-
270ponential suppression for eigenvalues less than 1. When the
271 weights are translation invariant ($W_{ij} = W_{i-j}$), the eigenvectors are
272 sines and cosine. In this case the network amplifies or suppresses
273 independently each Fourier component of the initial input pattern,
274 \mathbf{A} , by a factor equal to the corresponding eigenvalue of $(1 - \lambda)I$
275 $+ \lambda W$. For example, if the first eigenvalue of $(1 - \lambda)I + \lambda W$
276 is more than 1 (respectively less than 1), the first Fourier component
277 of the initial pattern of activity will be amplified (respectively sup-
278 pressed). Thus, W can be chosen such that the network amplifies
279 selectively the first Fourier component of the data while suppress-
280 ing the others.

281 As formulated, the activity in such a network would grow for-
282 ever. However, if we stop after a large yet fixed number of itera-
283 tions, the activity pattern will look like a cosine function of direc-
284 tion with a phase corresponding to the phase of the first Fourier
285 component of the data. The peak of the cosine provides the estimate
286 of direction. That estimate turns out to be the same as the one
287 provided by the population vector discussed above.

288 The unchecked exponential growth of a purely linear network
289 can be alleviated by adding a nonlinear term to act as gain control.
290 This type of network was proposed by Ben-Yishai, Bar-Or, and
291 Sompolinsky (1995) as a model of orientation selectivity.

292 Although such networks keep the estimate in a coarse code for-
293 mat, they suffer from two problems: it is not immediately clear
294 how to extend them to periodic variables, such as disparity, and
295 they are suboptimal, since they are equivalent to the population
296 estimator.

297 *Nonlinear Networks*

298 To obtain optimal performance, one needs a network that can im-
299 plement template matching with the correct template—the one used
300 by the ML estimator (see Figure 2B). This requires templates that
301 go beyond cosines to include curves that are consistent with the
302 tuning curves of the input units (see Figure 2B).

303 Nonlinear networks that admit line attractors have this property
304 (Deneve, Latham, and Pouget, 1999). In such networks, the line
305 attractors correspond to smooth hills of activity, with profiles de-
306 termined by the patterns of weights *and* the activation functions.
307 For a given activation function, it is therefore possible to select the
308 weights to optimize the profile of the stable state. Pouget et al.
309 (1998) demonstrated that this extra flexibility allows these net-
310 works to act as ML estimators (see Figure 3B).

311 More recent work by Deneve et al. (1999) has shown that the
312 ML property is preserved for a wide range of nonlinear activation
313 functions. In particular, this is true for networks using divisive
314 normalization, a nonlinearity believed to exist in cortical microcir-
315 cuitry. It is therefore possible that all cortical layers are close ap-
316 proximations to ML estimators.

317 **Estimating a Probability Distribution**

318 So far we have reviewed decoding methods in which only one value
319 is encoded at any given time and the only source of uncertainty
320 comes from the neuronal activity. Situations exist, however, in
321 which either (or both) of these assumptions are violated. For in-

322 stance, imagine that you are lost in Manhattan on a foggy day, but
323 you can see, faintly, the Empire State building and the Chrysler
324 building in the distance. Because of the poor visibility, the views
325 of these landmarks are not sufficient to specify your exact position,
326 but they are enough to provide a rough idea of where you are
327 (Harlem versus Little Italy). In this situation, it would be desirable
328 to compute the probability distribution of your location given that
329 you are seeing the landmarks; i.e., compute $P(\theta|w)$ where θ is the
330 position (now a two-dimensional vector) in Manhattan and w rep-
331 represents the views of the buildings. Here, the uncertainty about θ
332 comes from the fact that you do not have enough information to
333 tell precisely where you are. In such a situation, the neurons could
334 encode the *probability distribution*, $P(\theta|w)$.

335 Because the encoded entity is a probability distribution rather
336 than a single value, we can no longer use either Equation 1 or
337 Equation 2 as a model for the responses of the neurons; these equa-
338 tions provide only the likelihood of θ , $P(\mathbf{A}|\theta)$. What we need in-
339 stead is a model that specifies the likelihood of the whole encoded
340 probability distribution, $P[\mathbf{A}|P(\theta|w)]$. Note that $P(\theta|w)$ plays the
341 same role as θ previously, which is to be expected, now that $P(\theta|w)$
342 is the encoded entity. It is beyond the scope of this discussion to
343 provide equations for such models, but examples can be found in
344 Zemel, Dayan, and Pouget (1998).

345 Since \mathbf{A} is now a code for the probability distribution, the rele-
346 vant quantity to estimate is $P(\theta|w)$, which we denote $\hat{P}(\theta|w)$. This
347 is still within the realm of estimation theory, so we can use the
348 same tools that we used for the simpler case, such as ML decoding
349 (see Zemel et al., 1998).

350 To see the difference between encoding a single value and en-
351 coding a probability distribution, it is helpful to consider what hap-
352 pens when the neurons are deterministic—that is, when the neu-
353 ronal noise goes to zero. In this case, the encoded variable can be
354 recovered with infinite precision, since the only source of uncer-
355 tainty, the neuronal noise, is gone. Thus the ML estimate would be
356 exactly equal to the encoded value, and the posterior distribution,
357 $P(\theta|\mathbf{A})$, would be a Dirac function centered at θ . If the activity
358 encodes a probability distribution, on the other hand, one would
359 recover the *distribution* with infinite precision. However, the un-
360 certainty about θ may still be quite large (as was the case in our
361 Manhattan example), potentially far from a Dirac function.

362 It is too early to tell whether neurons encode probability distri-
363 butions; more empirical as well as theoretical work is needed. But
364 if the cortex has the ability to represent probability distributions, it
365 might be possible to determine how, and whether, the brain per-
366 forms Bayesian inferences. Bayesian inference is a powerful
367 method for performing computation in the presence of uncertainty.
368 Many engineering applications rely on this framework to perform
369 data analysis or to control robots, and several studies are now sug-
370 gesting that the brain might be using such inferences for perception
371 and motor control (see, e.g., Knill and Richards, 1996).

372 Conclusions

373 Understanding how to decode patterns of neuronal activity is a
374 critical step toward developing theories of representation and com-
375 putation in the brain. This article concentrated on the simplest case,
376 a single variable encoded in the firing rates of a population of
377 neurons. There are two main approaches to this problem. In the
378 first, the population encodes a single value, and decoding can be
379 done with Bayesian or maximum likelihood estimators. The un-
380 derlying assumption in this case is that neuronal noise is the only
381 source of uncertainty. We also saw that within this framework, one
382 can design neural networks that perform decoding optimally. In the
383 second approach, the population encodes a full probability distri-
384 bution over the variable of interest. Here both the variable and its
385 uncertainty can be extracted from the population activity. This
386 scheme could be used to perform statistical inferences—a powerful
387 way to perform computations over variables whose value is not
388 known with certainty. The challenge for future work will be to
389 determine whether the brain uses this type of code, and, if so, to
390 understand how realistic neural circuits can perform statistical in-
391 ferences over probability distributions.

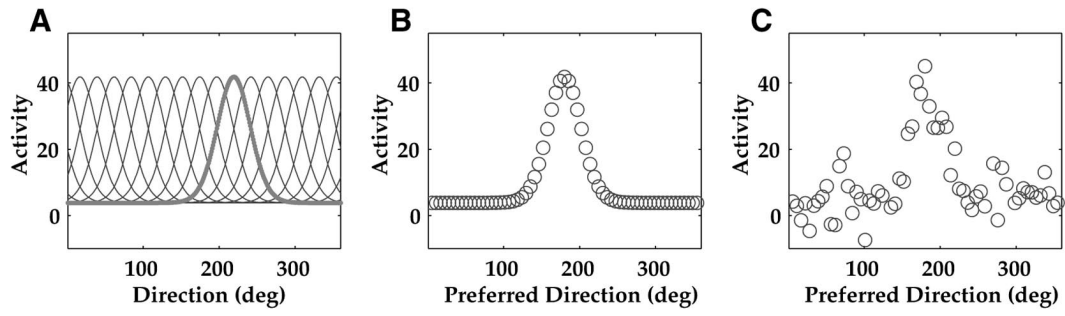
392 **Roadmap:** Neural Coding
393 **Related Reading:** Cortical Population Dynamics and Psychophysics; Mo-
394 tor Cortex, Coding and Decoding of Directional Operations

395 References

- 396 Ben-Yishai, R., Bar-Or, R. L., and Sompolinsky, H., 1995, Theory of ori-
397 entation tuning in visual cortex, *Proc. Natl. Acad. Sci. USA*, 92:3844–
398 3848.
- 399 Deneve, S., Latham, P. E., and Pouget, A., 1999, Reading population codes:
400 A neural implementation of ideal observers, *Nature Neurosci.*, 2:740–
401 745. ◆
- 402 Foldiak, P., 1993, The “ideal homunculus”: Statistical inference from neural
403 population responses, in *Computation and Neural Systems* (F. H. Eeck-
404 man and J. M. Bower, Eds.), Norwell, MA: Kluwer Academic, pp. 55–
405 60. ◆
- 406 Georgopoulos, A. P., Kalaska, J. F., Caminiti, R., and Massey, J. T., 1982,
407 On the relations between the direction of two-dimensional arm move-
408 ments and cell discharge in primate motor cortex. *J. Neurosci.*, 2:1527–
409 1537.
- 410 Knill, D. C., and Richards, W., 1996, *Perception as Bayesian Inference*,
411 New York: Cambridge University Press.
- 412 Paradiso, M. A., 1988, A theory of the use of visual orientation information
413 which exploits the columnar structure of striate cortex, *Biol. Cybern.*
414 58:35–49. ◆
- 415 Pouget, A., Zhang, K., Deneve, S., and Lathan, P., 1998, Statistically ef-
416 ficient estimation using population codes, *Neural computation*, 10:373–
417 401.
- 418 Pouget, A., Zemel, R. S., and Dayan, P., 2000, Information processing with
419 population codes, *Nature Rev. Neurosci.*, 1:125–132.
- 420 Salinas, E., and Abbott, L. F., 1994, Vector reconstruction from firing rate,
421 *J. Computat. Neurosci.*, 1:89–108. ◆
- 422 Sanger, T. D., 1996, Probability density estimation for the interpretation of
423 neural population codes, *J. Neurophysiol.*, 76:2790–2793.
- 424 Seung, H. S., and Sompolinsky, H., 1993, Simple model for reading neu-
425 ron population codes, *Proc. Natl. Acad. Sci. USA*, 90:10749–10753.
- 426 Zemel, R. S., Dayan, P., and Pouget, A., 1998, Probabilistic interpretation
427 of population code, *Neural Computat.*, 10:403–430. ◆
- 428 Zhang, K., Ginzburg, I., McNaughton, B. L., and Sejnowski, T. J., 1998,
429 Interpreting neuronal population activity by reconstruction: Unified
430 framework with application to hippocampal place cells. *J. Neurophysiol.*,
431 79:1017–1044.

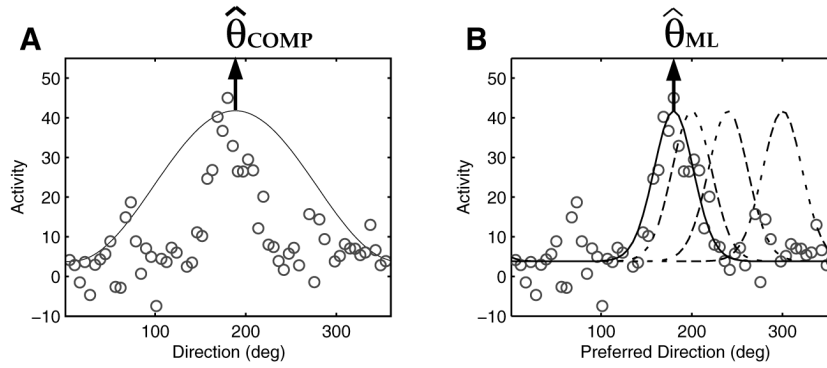
432

437



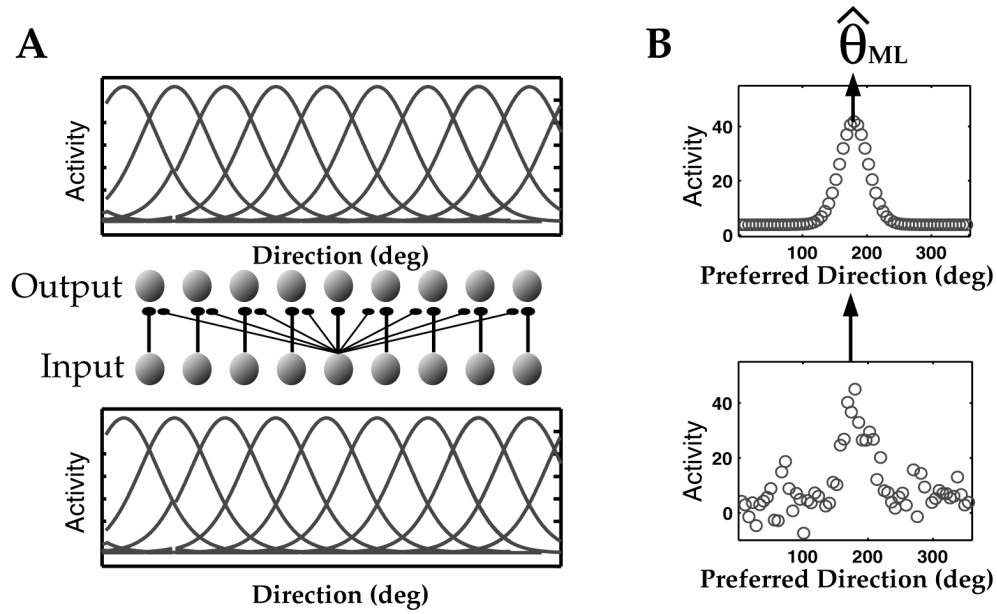
438

439 **Figure 1.** *A*, Idealized tuning curves for 16 direction-tuned neurons. *B*, Noiseless pattern of activity (○) from 64 simulated neurons with tuning curves like
440 the ones shown in *A*, when presented with a direction of 180°. The activity of each neuron is plotted at the location of its preferred direction. *C*, Same as *B*,
441 but in the presence of Gaussian noise.

444 $\hat{\nu}(\theta | I) ? (v2)$ 

447
448 **Figure 2.** *A*, The population vector estimator uses the phase of the first Fourier component of the input pattern (solid line) as an estimate of direction. It is
449 equivalent to fitting a cosine function to the input. *B*, The maximum likelihood estimate is found by moving an "expected" hill of activity (dashed line) until
450 the squared distance with the data is minimized (solid line).

454



455

456 **Figure 3.** A, A set of units with broad tuning to a sensory variable (in this case direction) projects to another set of units also broadly tuned to the same
 457 variable. This type of mapping between population codes is very common throughout the brain. In this particular network, the output layer is fully intercon-
 458 nected with lateral connections, and receives feedforward connections from the input layer. B, Temporal evolution of the activity in the output layer for a
 459 nonlinear network. The activity in the output layer is initiated with a noisy hill generated by the input units (bottom). For an appropriate choice of weights
 460 and activation function, these activities converge eventually to a smooth hill (top), which peaks close to the location of the maximum likelihood estimate of
 462 direction, $\hat{\theta}_{ML}$. This network is performing the template-matching procedure used in maximum likelihood and illustrated in Figure 2B.
 463